

pubs.acs.org/JPCL Letter

Influence of Substrate-Induced Charge Doping on Defect-Related Excitonic Emission in Monolayer MoS₂

Kyle T. Munson, Riccardo Torsi, Shreya Mathela, Maxwell A. Feidler, Yu-Chuan Lin, Joshua A. Robinson,* and John B. Asbury*



Cite This: J. Phys. Chem. Lett. 2024, 15, 7850-7856



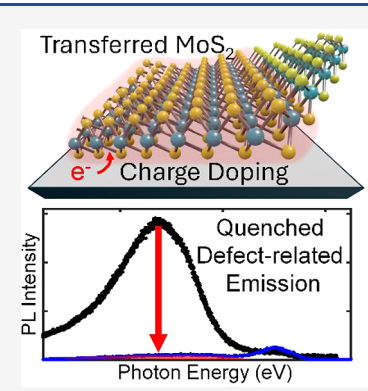
ACCESS

III Metrics & More

Article Recommendations

Supporting Information

ABSTRACT: Many applications of transition metal dichalcogenides (TMDs) involve transfer to functional substrates that can strongly impact their optical and electronic properties. We investigate the impact that substrate interactions have on free carrier densities and defect-related excitonic (X^D) emission from MoS_2 monolayers grown by metal—organic chemical vapor deposition. C-plane sapphire substrates mimic common hydroxyl-terminated substrates. We demonstrate that transferring MoS_2 monolayers to pristine c-plane sapphire dramatically increases the free electron density within MoS_2 layers, quenches X^D emission, and accelerates exciton recombination at the optical band edge. In contrast, transferring MoS_2 monolayers onto inert hexagonal boron nitride (h-BN) has no measurable influence on these properties. Our findings demonstrate the promise of utilizing substrate engineering to control charge doping interactions and to quench broad X^D background emission features that can influence the purity of single photon emitters in TMDs being developed for quantum photonic applications.



ransition metal dichalcogenide (TMD) semiconductors show promise in atomically thin field effect transistors (FETs),^{1,2} light-emitting diodes,³ and quantum photonic devices^{4,5} because of their high carrier mobilities at ultrathin (<5 nm) channel lengths, 1,6,7 direct bandgaps at the monolayer level,8 and controllable valley polarizations.5,9,10 Large-area TMDs with controlled layer thicknesses can be grown using metal-organic chemical vapor deposition (MOCVD) and other nonequilibrium synthesis methods. ^{2,11,12} However, chalcogen vacancies, ^{13,14} substitutional impurities, ¹² and grain boundaries¹⁵ are widely observed in TMDs grown using these techniques. 16,17 In particular, chalcogen vacancies are prevalent in MOCVD-grown TMDs due to their low formation energy in vacuum, resulting in chalcogen vacancy defect densities on the order of 10^{12} to 10^{13} cm⁻². These defects hinder carrier transport within the TMD layer and limit the performance of TMD-based FETs.

Additionally, several reports have observed photon emission from excitons trapped at defect sites in TMDs such as MoS₂, ^{14,19} WS₂, ²⁰ MoSe₂, ²¹ and WSe₂. ²² In fact, investigators have demonstrated narrow single photon ^{4,23–25} and circularly polarized ²² emission from defects in TMDs, indicating that these states may find uses in quantum photonic devices. ⁴ In addition to narrow single photon emission, investigators have also observed broad defect-related (X^D) emission in TMDs, ^{14,19,20} which can reduce the purity and correlation score of single photon emitters that overlap spectrally. ²⁶ Furthermore, X^D emission features are commonly used as a metric to determine the presence of defects within the TMD layer. ^{14,19,20,27,28} For example, researchers have observed

positive correlations between X^D emission and sulfur vacancy defects in CVD-grown WS₂ flakes using photoluminescence (PL) spectroscopy and Z-contrast scanning transmission electron microscopy (Z-STEM). Emission from defect states also has been observed following the intentional creation of sulfur vacancies by Ar^+ plasma or electron beam irradiation. 22

In addition to defects, the properties of TMDs are influenced by their underlying substrates. Fabricating TMD devices often involves transferring TMDs from their growth substrates, such as sapphire, to device-relevant substrates, such as SiO₂/Si or hexagonal boron nitride (h-BN).^{2,31,32} Significant progress has been made in developing methods for transferring large-area TMD films without degrading material quality. 2,32,33 However, substrate interactions following sample transfer can unintentionally dope the TMD layer, 15,24,31,34-36 making it challenging to predict and control the electronic and photonic properties of TMDs in device applications. For example, excess carriers from substrates can influence band bending and contact resistances at TMD/metal interfaces.³⁷ Additionally, inadvertent doping can suppress the radiative decay of excitons, 15 hindering the use of TMDs in light-emitting applications. For example, transferring MoS₂ monolayers to

Received: May 28, 2024 Revised: July 18, 2024 Accepted: July 23, 2024 Published: July 25, 2024





 ${\rm SiO_2/Si}$ quenched PL from excitons at the material's optical band-edge by increasing n-type doping and trion formation. Investigators attributed this doping to charged impurities at the ${\rm MoS_2/SiO_2/Si}$ interface. Similarly, the hydroxylation and hydration of sapphire substrates resulted in increased charge transfer (> 10^{13} e $^-/{\rm cm}^2$) to ${\rm MoS_2}$ and ${\rm WS_2}$ monolayers transferred to the sapphire. Sis, These and other studies highlight the impact of substrate interactions on charge doping in TMDs. However, the impact of this doping on excited-state processes occurring at TMD defect sites remains an open area of research. Such knowledge is critical for developing TMD devices with controlled and predictable defect densities and optical, electronic, and transport properties.

In this work, we demonstrate that substrate-induced doping affects X^D emission and recombination in MoS₂ monolayers grown by MOCVD. PL measurements reveal that transferring MoS₂ monolayers to pristine c-plane oriented sapphire (csapphire) substrates, which did not undergo the MOCVD process, dramatically increases the density of free electrons within the MoS₂ monolayer. We attribute this enhancement in electron doping to charge transfer interactions between MoS₂ and Al-OH groups at the sapphire's surface. Temperaturedependent PL measurements show that electron doping from pristine c-sapphire quenches X^D emission and accelerates recombination at the MoS₂ optical band-edge. Conversely, MoS₂ films transferred to chemically inert h-BN do not exhibit these effects. These results illustrate the interplay between substrate-induced doping, X^D emission, and recombination in TMDs and provide a framework for characterizing TMD films following sample transfer. Importantly, this work suggests that controlling charge doping interactions from substrates can aid the development of future TMD-based quantum photonic devices by quenching emission from X^D states that overlap spectrally with single photon emitters.^{4,23-25}

MoS₂ films are grown on c-sapphire substrates using a MOCVD process that yields MoS₂ monolayers with low bilayer coverage (Figure S1). 13 We transfer the MoS₂ films from their growth substrates by coating the MoS2 layer with poly(methyl methacrylate) (PMMA) and then placing thermal release tape (TRT) on the PMMA/MoS₂/c-sapphire stack. This stack is placed in deionized water and sonicated to remove PMMA/MoS₂ from the growth substrate. After drying, we stamp the TRT/PMMA/MoS₂ stack onto a pristine csapphire wafer that did not go through the MOCVD process. The sapphire wafer mimics the types of hydroxyl terminated substrates commonly used in device applications of TMD materials. The TRT and PMMA above the MoS₂ are then removed by heating and exposing the sample to acetone. Spatially resolved PL measurements (Figure S2) of a transferred MoS₂ film on c-sapphire show uniform emission from the MoS₂ layer over an \sim 40 μ m² area, indicating that the transfer process does not noticeably damage the MoS₂ layer.

Transferring MoS₂ from its growth substrate can have a pronounced effect on doping in the MoS₂ layer. This effect is evident when assessing the PL spectra (Figure 1a,b) of asgrown and transferred MoS₂ films on c-sapphire collected at room temperature following optical excitation at 445 nm (2 kW/cm²). Compared to as-grown MoS₂, PL in the transferred film is quenched and red-shifted by ~35 meV (Figure 1b). These changes in PL are consistent with enhanced trion formation and associated nonradiative recombination in the transferred film. ^{13,38} To determine the contribution of trions (red dashed line) and neutral A-excitons (blue dashed line) to

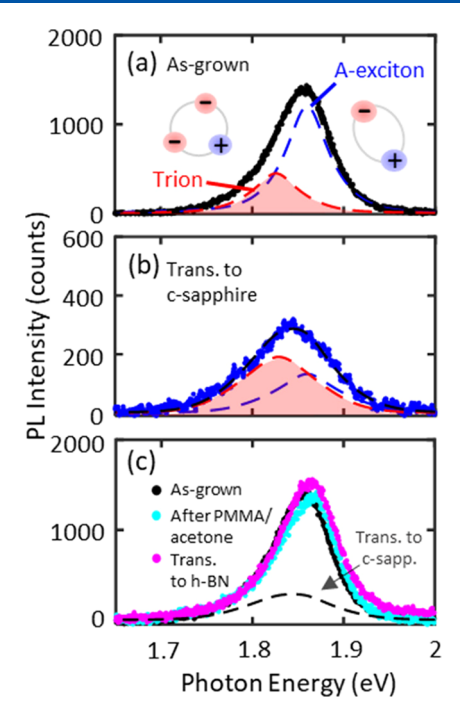


Figure 1. Emission properties of as-grown and transferred MoS_2 films. (a) Room temperature photoluminescence (PL) spectrum of an as-grown MoS_2 film synthesized onto c-plane sapphire using MOCVD. (b) PL spectrum of a MoS_2 film transferred to pristine c-plane sapphire. The spectra are fit with two pseudo-Voigt curves centered at ~1.84 and 1.88 eV to determine the contribution of trions (red dashed line) and A-excitons (blue dashed line) to the overall emission. Increased trion formation is observed in the transferred MoS_2 film on c-sapphire. (c) PL spectrum of an as-grown film compared to the PL spectrum of the same film after being coated with PMMA and subsequently having the PMMA washed off with acetone. The PL spectrum of a MoS_2 transferred to h-BN is also shown. We observe no significant changes in PL after exposure to PMMA/ acetone or transfer to h-BN.

the overall emission, the spectra are fit with two pseudo-Voigt curves centered at ~1.84 and 1.88 eV (Figure 1). Using a mass action model (see Supporting Information), 13,34 we find from the intensity ratio of the trion and A-exciton peaks that the electron density within the MoS₂ films is quadrupled from $\sim 8.4 \times 10^{12} \text{ e}^{-/\text{cm}^2} \text{ to } \sim 3.0 \times 10^{13} \text{ e}^{-/\text{cm}^2} \text{ after being}$ transferred to a pristine c-sapphire substrate. We acknowledge that in this analysis, the radiative decay rates for A-excitons $(\gamma_{\rm ex})$ and trions $(\gamma_{\rm tr})$, as well as the trion binding energy $(E_{\rm b})$, are assumed to be constant for both as-grown and transferred samples. It is possible that charge doping could change these rates and reduce $E_{\rm b}$ by modifying the screening of electron hole interactions in the MoS_2 . ³⁹ A reduction in E_b would result in higher estimates for carrier concentrations obtained from the mass-action model for a given trion/A-exciton PL intensity ratio. However, we do not observe differences in E_b (i.e., the energy spacing between trion and A-exciton PL) following sample transfer (Figure 1). Additionally, investigators have demonstrated that the radiative lifetimes of trions and Aexcitons in MoSe₂ monolayers are not notably affected by changes in background electron density induced by an applied electric field. Therefore, we do not anticipate significant changes in γ_{ex} and γ_{tr} between the as-grown and transferred

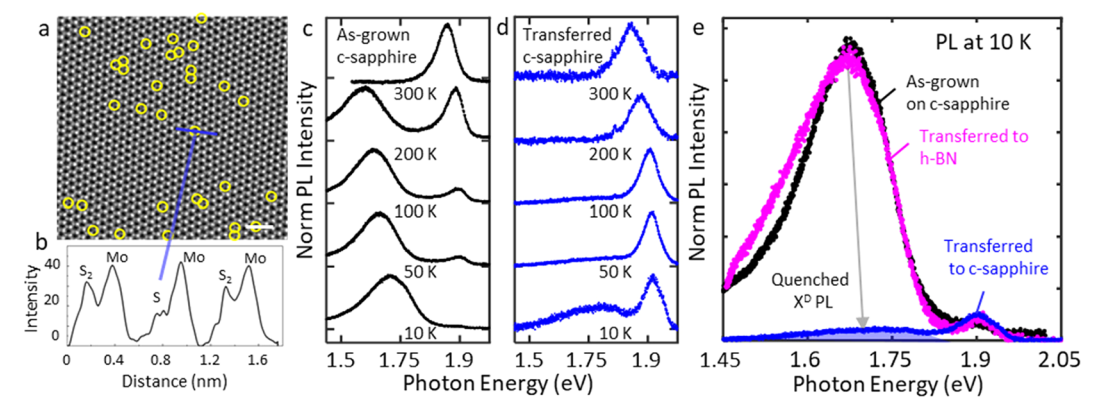


Figure 2. Influence of substrate-induced doping on defect-related emission in MoS_2 monolayers. (a) Atomic resolution STEM image of an asgrown MoS_2 film highlighting the presence of sulfur-site defects (yellow circles) within the material. The scale bar is 1 nm. (b) Line profile depicting the relative Z-intensity of MoS_2 , and S (sulfur-site defect). Temperature-dependent PL spectra of (c) as-grown and (d) transferred MoS_2 films on c-sapphire. (e) PL spectra of as-grown and transferred MoS_2 films collected at 10 K. The spectra are normalized to the maximum free exciton (trion/A-exciton) PL intensity at \sim 1.9 eV. Quenched X^D emission following transfer to c-sapphire is due to enhanced charge transfer interactions at the MoS_2 /c-sapphire interface. We do not observe quenched X^D emission following transfer to h-BN substrates that lack such interactions.

Identifying the origins of increased electron doping and trion formation in films transferred to pristine c-sapphire is critical for developing design rules that describe how to control the photonic and electronic properties of TMDs. We confirm that the PL of MoS₂ is not significantly affected by the chemicals used during the transfer process (PMMA, acetone) by measuring the PL (Figure 1c) of an as-grown MoS₂ film that was coated with PMMA and subsequently had the PMMA washed off with acetone. Within our experimental precision, we also observe no changes in PL (Figures 1c and S3) after transferring MoS₂ films to chemically inert h-BN, which forms a Van Der Waals interface with MoS2 free of step edges, dangling bonds, and charge transfer interactions.³⁴ results emphasize that changes in electron doping and PL following transfer to c-sapphire (Figure 1b) do not arise from the unintentional creation of n-type sulfur vacancies⁴⁰ during the transfer process, as such vacancy creation would also occur in samples transferred to h-BN. Additionally, several studies have demonstrated that the local dielectric environment around TMDs can influence PL and trion formation rates. 41,42 Specifically, MoS₂ films submerged in nonionizing organic solvents with high dielectric constants (e.g., methanol) exhibited greater PL intensities and lower trion formation rates compared to MoS₂ films submerged in organic solvents with low dielectric constants (e.g., hexanes).42 The authors attributed these changes to reduced dielectric screening between electrons and holes in the latter. However, h-BN has a lower dielectric constant ($\epsilon \sim 3$) compared to sapphire $(\epsilon \sim 9-10)$. Therefore, our PL results (Figure 1c) suggest that changes in dielectric environment are not the primary cause of increased trion formation in MoS2 films transferred to c-sapphire, as we would anticipate these films to exhibit lower trion formation versus films transferred to h-BN if comparing the substrates' dielectric constants alone.

These results indicate that electron doping following transfer to c-sapphire is due to increased charge transfer interactions at the sapphire surface. Recent reports show that a layer of sulfur atoms forms on the surface of sapphire substrates during MOCVD growth of MoS₂ when using H₂S as a sulfur source. ⁴⁸ This sulfur layer is believed to insulate as-grown MoS₂ films from charge transfer interactions with the underlying sapphire

substrate.⁴⁵ Conversely, the hydroxylation and hydration of pristine c-sapphire substrates in ambient conditions cause their surfaces to exhibit Al–OH groups that are Lewis bases (electron donors).^{35,46} Investigators have demonstrated that removing Al–OH groups and water using sulfuric acid can reduce electron doping at the TMD/sapphire interface and increase the PL intensity of the TMD layer.³⁶ Therefore, we conclude that increased electron doping following transfer to pristine c-sapphire is due to enhanced charge transfer interactions with Al–OH groups and trapped water at the substrate's surface.

Substrate-induced charge doping quenches emission from X^D states in MoS₂. To date, investigators have primarily relied on scanning probe and electron microscopy measurements to investigate the atomic structure and defect densities of TMDs. 47-51 For example, Z-STEM measurements (Figure 2a,b) of a MOCVD-grown MoS2 monolayer transferred to a TEM grid using a PMMA-mediated wet-transfer method (see Supporting Information) indicate the presence of sulfur vacancies (yellow circles) within the material. Analysis of the STEM image yields a sulfur vacancy concentration of \sim 3.3 \times 10¹³ cm⁻², which is consistent with prior defect analysis of MOCVD-grown MoS₂. 13 We note that the sulfur vacancies observed in our STEM image are likely filled with oxygen or carbohydrate (-CH) species, as reported in previous studies. 47,48,52,53 Therefore, we collectively refer to these vacancies as sulfur-site defects in the following discussion. Unlike STEM measurements, which require extensive sample preparation and have a limited field of view (~10's nm), PL spectroscopy offers a quicker and more efficient way to characterize defects in TMDs over large areas. The PL spectra of an as-grown MoS₂ film collected from 10 to 300 K following optical excitation at 445 nm are displayed in Figure 2c.

At temperatures \leq 200 K, the spectra exhibit emission from freely diffusing neutral A-excitons and trions at the optical band edge of MoS₂, which we refer to as "free excitons" in the following discussion. We also observe broad X^D emission, which has been observed previously in MoS₂ films¹³ and other TMDs. ^{14,17,19,54} The exact origin of broad X^D emission in TMDs is a subject of debate. However, it likely originates from a combination of excitons trapped at sulfur-site defects and

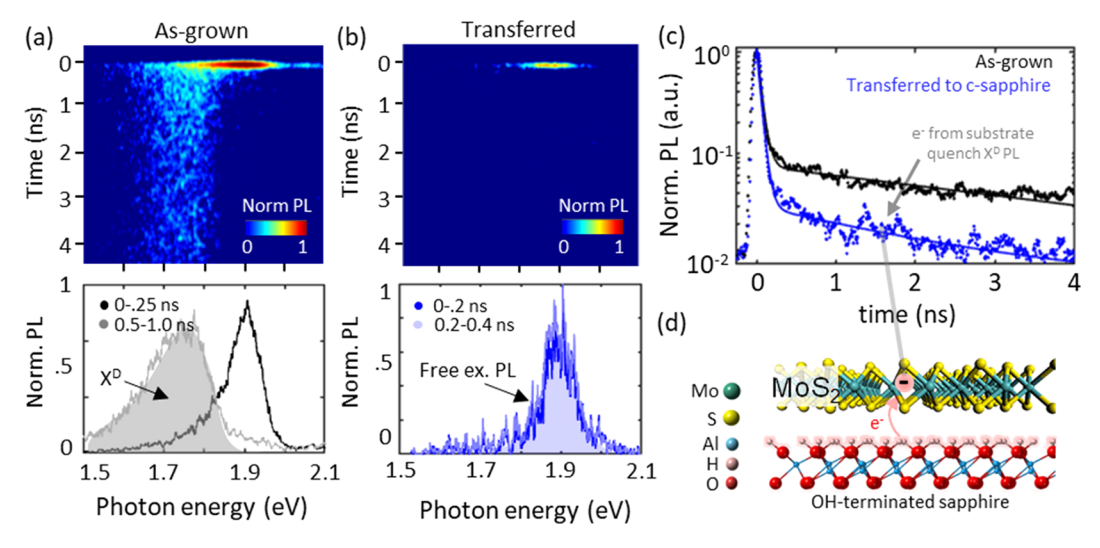


Figure 3. Influence of substrate on exciton recombination in MoS₂ monolayers. (a) Top: Streak camera image of an as-grown MoS₂ film measured at 10 K following optical excitation at 445 nm. Bottom: PL spectra obtained by integrating the film's streak camera image between 0 and 0.25 and 0.5–1.0 ns. (b) Top: Streak camera image of a MoS₂ film transferred to c-sapphire measured under identical conditions. Bottom: PL spectra of the transferred film collected by integrating the film's PL at 0–0.20 and 0.2–0.40 ns time delays. (c) Exciton recombination kinetics obtained by integrating the streak camera images of the as-grown and transferred MoS₂ films between 1.7 and 1.9 eV. (d) Model of the MoS₂/ pristine c-sapphire interface.

interactions between excitons and molecules adsorbed at these defect sites.⁵⁵ Compared to as-grown MoS₂ (Figures 2c and S4), MoS₂ films transferred to pristine c-sapphire exhibit markedly reduced X^D emission (Figure 2d) and higher trion/ A-exciton PL ratios (Figure S5), consistent with the observation of increased electron doping following transfer to c-sapphire obtained from room temperature measurements (Figure 1). The observation of quenched X^D emission is illustrated further by comparing the 10 K PL spectra normalized to the maximum free exciton PL intensity (Figure 2e) of an "As-grown" MoS2 monolayer with the equivalent sample transferred to c-sapphire. Importantly, we do not observe quenched XD emission in a MoS2 film exposed to PMMA and acetone, which are used during the transfer process (Figure S6). Therefore, we rule out the passivation of sulfur-site defects by residual polymer and solvent molecules as the origin of quenched X^D emission in the transferred MoS₂ film. Finally, we measured all samples under identical conditions in high vacuum ($\sim 10^{-6}$ Torr), indicating that X^D quenching does not arise from changes in adsorbate interactions, as we expect all samples to exhibit similar interactions with adsorbate species. Rather, these results indicate that X^D emission is quenched in the MoS₂ monolayer transferred to pristine c-sapphire because of the ~4-fold increase of the free electron density introduced by interactions with the hydroxyl-terminated c-sapphire interface. This doping enhances nonradiative recombination at defect sites due to trion formation, leading to quenching of the XD emission in MoS₂ films transferred to pristine c-sapphire (Figure 2d). 28,56 An alternate mechanism of carrier-induced quenching of X^D emission may involve movement of the MoS₂ Fermi level closer to the material's conduction band edge. Such a shift of the Fermi level would reduce the density of neutral defect states accessible for exciton trapping and radiative X^D recombination.¹⁷ In either case, these findings demonstrate significant alteration of the electronic and optical properties of the MoS₂ monolayers due to substrate-induced changes in free electron density.

We further confirm that substrate-induced charge doping quenches emission from XD states by comparing in Figure 2e the low-temperature PL spectra measured of an as-grown MoS₂ monolayer on its original sapphire growth substrate with a MoS₂ monolayer transferred to inert h-BN. The comparison reveals minimal variations in X^D emission between the samples at 10 K. We note that transferring MoS₂ films to h-BN does not increase electron doping within the MoS2 layer (Figure 1c). The invariance of the low temperature PL spectra in this comparison highlights the impact that substrate-induced doping of the hydroxyl terminated c-plane sapphire has on X^D emission in MoS₂ monolayers that is not observed of MoS₂ monolayers transferred to h-BN. This result further suggests that possible strain release caused by transferring MoS₂ films away from their growth substrates 57 does not lead to XD quenching, as such strain release would occur in MoS2 films transferred to both c-sapphire and h-BN.

These results suggest that doping from the substrate may mask the presence of defects within TMDs if X^D emission is used as the sole indicator of material quality, particularly when comparing TMD films transferred away from their growth substrates. Fortunately, such substrate-induced doping interactions can be identified by characterization of the electron concentration using trion/A-exciton PL peak ratios measured at room temperature as illustrated in Figure 1 before evaluating X^D emission. Careful assessment of both X^D emission and trion/A-exciton PL peaks allows substrate-induced doping effects to be disentangled from the material's underlying defect distribution. Additionally, pairing temperature-dependent PL studies of TMDs with atomic-scale characterization methods can further help facilitate the accurate interpretation of a TMD's PL spectra in relation to its underlying defect characteristics.

Monitoring the time-dependent emission properties of MoS_2 films provides further insight into the interplay between substrate-induced charge doping and defect characteristics within the material. We show a streak camera image of PL from an as-grown MoS_2 film collected at 10 K following optical

excitation at 445 nm (5 pJ/pulse) in Figure 3a. Our streak camera's instrument response function (~45 ps) is shown in Figure S7. Analysis of the image reveals that PL from free excitons (A-excitons and trions) at the optical band-edge of MoS_2 (~1.9 eV) dominates at early time delays (<0.25 ns). On later time scales (>0.25 ns), the PL redshifts toward the X^D emission band at ~1.7 eV. Time-integrated PL spectra (Figure 3a) obtained by integrating the streak camera image at early \sim 0-.25 and late \sim 0.50-1.0 ns time delays illustrate this spectral evolution. In studies of inorganic quantum wells and other disordered systems at low temperatures (<50 K), 58,59 similar shifts in PL are commonly observed and attributed to the relaxation of excitons into unoccupied defect states. Therefore, the spectral evolution of PL from the as-grown film indicates a distribution of defects and impurities with energies below the optical bandgap of the material. Conversely, emission (Figures 3b and S8) from MoS₂ films transferred to csapphire is dominated by trions and predominately occurs at the MoS₂ optical band-edge, decaying on earlier time scales compared to the as-grown analog (Figure 3a). This observation is illustrated further by comparing PL decay traces (Figure 3c) of the as-grown and transferred MoS₂ films obtained by integrating their PL between 1.7 and 1.9 eV. We used biexponential functions to fit the decay's fast (free exciton) and slow (XD) components and show the best-fit parameters in Table S1. From the fits, we obtain average PL lifetimes of 0.34 and 0.10 ns for as-grown and transferred MoS₂ films on c-sapphire, respectively. This result further supports the conclusion that substrate-induced electron doping enhances nonradiative recombination at defect sites and reduces the number of neutral defect states available for exciton trapping and X^D emission within MoS_2 (Figure 3d). Additionally, we note that compared to steady-state PL measurements collected with a continuous-wave laser (Figure 2d), the PL spectra of the transferred film obtained from timeresolved streak camera measurements (Figure 3b) are redshifted by ~20 meV and do not exhibit detectible X^D emission at \sim 1.65–1.7 eV. We speculate that this difference results from the removal of adsorbates at the MoS2 surface due to the higher peak power of the pulsed laser used for time-resolved measurements, which has been shown to red-shift MoS₂ PL and reduce X^D emission. 60,61

In conclusion, we examine the influence that substrate interactions and associated charge doping of MoS2 monolayers has on their free carrier densities and defect-related excitonic (XD) emission properties. Time- and temperature-resolved photoluminescence (PL) measurements reveal that transferring MoS₂ monolayers to hydroxyl terminated c-plane sapphire substrates, increases their free electron density, quenches broad X^D emission, and accelerates recombination in MoS₂ monolayers. The increased electron doping within the MoS₂ layer is likely due to the c-plane sapphire surface exhibiting electron-donating Al-OH groups. Importantly, these marked changes of the electronic and excited state optical properties of the MoS₂ monolayers do not occur when the monolayers are transferred onto hexagonal boron nitride (h-BN) substrates that form inert Van-Der Waals interfaces with MoS₂. Our findings highlight the potential to use substrate engineering to understand and control the electronic properties of TMDs and to tune the photonic properties of their defects. For example, applications of TMDs in quantum photonic devices are hindered by broad X^D emission that reduces the purity and correlation scores of single photon

emitters within the TMDs. 26,62 However, the ability to quench emission from X^D states via substrate engineering may be a promising approach to avoid this complication and preserve the properties of TMD single photon emitters in device-relevant architectures. Finally, our findings emphasize the need to carefully evaluate defect densities and substrate doping effects using atomic-scale characterization and PL techniques before using X^D emission as a metric of TMD sample quality.

ASSOCIATED CONTENT

Supporting Information

The Supporting Information is available free of charge at https://pubs.acs.org/doi/10.1021/acs.jpclett.4c01578.

Detailed experimental procedures, Raman spectra of MoS_2 monolayer samples, photoluminescence spectra and optical images of MoS_2 samples, and mass action model to determine electron density from photoluminescence spectra (PDF)

Transparent Peer Review report available (PDF)

AUTHOR INFORMATION

Corresponding Authors

Joshua A. Robinson — Department of Materials Science and Engineering, The Pennsylvania State University, University Park, Pennsylvania 16802, United States; Department of Chemistry, Materials Research Institute, and Department of Physics, The Pennsylvania State University, University Park, Pennsylvania 16802, United States; Orcid.org/0000-0002-1513-7187; Email: jar403@psu.edu

John B. Asbury — Department of Materials Science and Engineering, The Pennsylvania State University, University Park, Pennsylvania 16802, United States; Department of Chemistry, The Pennsylvania State University, University Park, Pennsylvania 16802, United States; orcid.org/0000-0002-3641-7276; Email: jasbury@psu.edu

Authors

Kyle T. Munson – Department of Materials Science and Engineering, The Pennsylvania State University, University Park, Pennsylvania 16802, United States; ⊚ orcid.org/ 0009-0001-6099-8349

Riccardo Torsi — Department of Materials Science and Engineering, The Pennsylvania State University, University Park, Pennsylvania 16802, United States; orcid.org/0000-0001-7748-1074

Shreya Mathela — Department of Chemistry, The Pennsylvania State University, University Park, Pennsylvania 16802, United States

Maxwell A. Feidler – Department of Materials Science and Engineering, The Pennsylvania State University, University Park, Pennsylvania 16802, United States

Yu-Chuan Lin — Department of Materials Science and Engineering, National Yang Ming Chiao Tung University, Hsinchu City 300, Taiwan; orcid.org/0000-0003-4958-5073

Complete contact information is available at: https://pubs.acs.org/10.1021/acs.jpclett.4c01578

Notes

The authors declare the following competing financial interest(s): J.B.A. owns equity in Magnitude Instruments, which has an interest in this project. His ownership in this

company has been reviewed by the Pennsylvania State University Individual Conflict of Interest Committee and is currently being managed by the University.

ACKNOWLEDGMENTS

K.T.M., J.A.R., and J.B.A. acknowledge funding from the U.S. National Science Foundation Major Research Instrumentation Program for development of the steady-state and time-resolved PL microscope through Award DMR-1826790. R.T., Y.-C.L., and J.A.R. acknowledge funding from NEWLIMITS, a center in nCORE as part of the Semiconductor Research Corporation (SRC) Program sponsored by NIST through Award 70NANB17H041. R.T. and J.A.R. also acknowledge funding from NSF ECCS- 2202280 and NSF DMR-2039351.

REFERENCES

- (1) Yu, Z.; Ong, Z. Y.; Li, S.; Xu, J.-B.; Zhang, G.; Zhang, Y. W.; Shi, Y.; Wang, X. Analyzing the Carrier Mobility in Transition-Metal Dichalcogenide MoS₂ Field-Effect Transistors. *Adv. Funct. Mater.* **2017**, 27, No. 1604093.
- (2) Sebastian, A.; Pendurthi, R.; Choudhury, T. H.; Redwing, J. M.; Das, S. Benchmarking Monolayer MoS₂ and WS₂ Field-Effect Transistors. *Nat. Commun.* **2021**, *12*, 693.
- (3) Wang, C.; Yang, F.; Gao, Y. The Highly-Efficient Light-Emitting Diodes Based on Transition Metal Dichalcogenides: From Architecture to Performance. *Nanoscale Adv.* **2020**, *2*, 4323–4340.
- (4) Klein, J.; Lorke, M.; Florian, M.; Sigger, F.; Sigl, L.; Rey, S.; Wierzbowski, J.; Cerne, J.; Müller, K.; Mitterreiter, E.; Zimmermann, P.; Taniguchi, T.; Watanabe, K.; Wurstbauer, U.; Kaniber, M.; Knap, M.; Schmidt, R.; Finley, J. J.; Holleitner, A. W. Site-Selectively Generated Photon Emitters in Monolayer MoS₂ Via Local Helium Ion Irradiation. *Nat. Commun.* **2019**, *10*, 2755.
- (5) Chakraborty, C.; Kinnischtzke, L.; Goodfellow, K. M.; Beams, R.; Vamivakas, A. N. Voltage-Controlled Quantum Light from an Atomically Thin Semiconductor. *Nat. Nanotechnol.* **2015**, *10*, 507–511.
- (6) Liu, Y.; Duan, X.; Shin, H.-J.; Park, S.; Huang, Y.; Duan, X. Promises and Prospects of Two-Dimensional Transistors. *Nature* **2021**, *591*, 43–53.
- (7) Radisavljevic, B.; Radenovic, A.; Brivio, J.; Giacometti, V.; Kis, A. Single-Layer MoS₂ Transistors. *Nat. Nanotechnol.* **2011**, *6*, 147–150.
- (8) Splendiani, A.; Sun, L.; Zhang, Y.; Li, T.; Kim, J.; Chim, C.-Y.; Galli, G.; Wang, F. Emerging Photoluminescence in Monolayer MoS₂. *Nano Lett.* **2010**, *10*, 1271–1275.
- (9) Feng, S.; Cong, C.; Konabe, S.; Zhang, J.; Shang, J.; Chen, Y.; Zou, C.; Cao, B.; Wu, L.; Peimyoo, N.; Zhang, B.; Yu, T. Engineering Valley Polarization of Monolayer WS₂: A Physical Doping Approach. *Small* **2019**, *15*, No. 1805503.
- (10) Mak, K. F.; He, K.; Lee, C.; Lee, G. H.; Hone, J.; Heinz, T. F.; Shan, J. Tightly Bound Trions in Monolayer MoS₂. *Nat. Mater.* **2013**, 12, 207–211.
- (11) Zhang, X.; Choudhury, T. H.; Chubarov, M.; Xiang, Y.; Jariwala, B.; Zhang, F.; Alem, N.; Wang, G.-C.; Robinson, J. A.; Redwing, J. M. Diffusion-Controlled Epitaxy of Large Area Coalesced WSe₂ Monolayers on Sapphire. *Nano Lett.* **2018**, *18*, 1049–1056.
- (12) Lin, Y.-C.; Jariwala, B.; Bersch, B. M.; Xu, K.; Nie, Y.; Wang, B.; Eichfeld, S. M.; Zhang, X.; Choudhury, T. H.; Pan, Y.; Addou, R.; Smyth, C. M.; Li, J.; Zhang, K.; Haque, A. M.; Fölsch, S.; Feenstra, R. M.; Wallace, R. M.; Cho, K.; Fullerton-Shirey, S. K.; Redwing, J. M.; Robinson, J. A. Realizing Large-Scale, Electronic-Grade Two-Dimensional Semiconductors. *ACS Nano* **2018**, *12*, 965–975.
- (13) Torsi, R.; Munson, K. T.; Pendurthi, R.; Marques, E.; Van Troeye, B.; Huberich, L.; Schuler, B.; Feidler, M.; Wang, K.; Pourtois, G.; Das, S.; Asbury, J. B.; Lin, Y.-C.; Robinson, J. A. Dilute Rhenium Doping and Its Impact on Defects in MoS₂. ACS Nano **2023**, 17, 15629–15640.

- (14) Tongay, S.; Suh, J.; Ataca, C.; Fan, W.; Luce, A.; Kang, J. S.; Liu, J.; Ko, C.; Raghunathanan, R.; Zhou, J.; Ogletree, F.; Li, J.; Grossman, J. C.; Wu, J. Defects Activated Photoluminescence in Two-Dimensional Semiconductors: Interplay between Bound, Charged and Free Excitons. *Sci. Rep.* **2013**, *3*, 2657.
- (15) Zhang, K.; Borys, N. J.; Bersch, B. M.; Bhimanapati, G. R.; Xu, K.; Wang, B.; Wang, K.; Labella, M.; Williams, T. A.; Haque, M. A.; Barnard, E. S.; Fullerton-Shirey, S.; Schuck, P. J.; Robinson, J. A. Deconvoluting the Photonic and Electronic Response of 2D Materials: The Case of MoS₂. Sci. Rep. 2017, 7, 16938.
- (16) Liang, Q.; Zhang, Q.; Zhao, X.; Liu, M.; Wee, A. T. S. Defect Engineering of Two-Dimensional Transition-Metal Dichalcogenides: Applications, Challenges, and Opportunities. *ACS Nano* **2021**, *15*, 2165–2181.
- (17) Rhodes, D.; Chae, S. H.; Ribeiro-Palau, R.; Hone, J. Disorder in Van Der Waals Heterostructures of 2d Materials. *Nat. Mater.* **2019**, *18*, 541–549.
- (18) Noh, J.-Y.; Kim, H.; Kim, Y.-S. Stability and Electronic Structures of Native Defects in Single-Layer MoS₂. *Phys. Rev. B* **2014**, 89, No. 205417.
- (19) Goodman, A. J.; Willard, A. P.; Tisdale, W. A. Exciton Trapping Is Responsible for the Long Apparent Lifetime in Acid-Treated MoS₂. *Phys. Rev. B* **2017**, *96*, No. 121404.
- (20) Carozo, V.; Wang, Y.; Fujisawa, K.; Carvalho, B. R.; Mccreary, A.; Feng, S.; Lin, Z.; Zhou, C.; Perea-López, N.; Elías, A. L.; Kabius, B.; Crespi, V. H.; Terrones, M. Optical Identification of Sulfur Vacancies: Bound Excitons at the Edges of Monolayer Tungsten Disulfide. *Sci. Adv.* 2017, 3, No. e1602813.
- (21) Wang, J.; Huang, J.; Li, Y.; Ding, K.; Jiang, D.; Dou, X.; Sun, B. Radiative and Non-Radiative Exciton Recombination Processes in a Chemical Vapor Deposition-Grown MoSe₂ Film. *J. Phys. Chem. C* **2022**, *126*, 15319–15326.
- (22) Moody, G.; Tran, K.; Lu, X.; Autry, T.; Fraser, J. M.; Mirin, R. P.; Yang, L.; Li, X.; Silverman, K. L. Microsecond Valley Lifetime of Defect-Bound Excitons in Monolayer WSe₂. *Phys. Rev. Lett.* **2018**, 121, No. 057403.
- (23) Sortino, L.; Zotev, P. G.; Phillips, C. L.; Brash, A. J.; Cambiasso, J.; Marensi, E.; Fox, A. M.; Maier, S. A.; Sapienza, R.; Tartakovskii, A. I. Bright Single Photon Emitters with Enhanced Quantum Efficiency in a Two-Dimensional Semiconductor Coupled with Dielectric Nano-Antennas. *Nat. Commun.* **2021**, *12*, 6063.
- (24) Klein, J.; Kerelsky, A.; Lorke, M.; Florian, M.; Sigger, F.; Kiemle, J.; Reuter, M. C.; Taniguchi, T.; Watanabe, K.; Finley, J. J.; Pasupathy, A. N.; Holleitner, A. W.; Ross, F. M.; Wurstbauer, U. Impact of Substrate Induced Band Tail States on the Electronic and Optical Properties of MoS₂. *Appl. Phys. Lett.* **2019**, *115*, No. 261603.
- (25) Klein, J.; Sigl, L.; Gyger, S.; Barthelmi, K.; Florian, M.; Rey, S.; Taniguchi, T.; Watanabe, K.; Jahnke, F.; Kastl, C.; Zwiller, V.; Jöns, K. D.; Müller, K.; Wurstbauer, U.; Finley, J. J.; Holleitner, A. W. Engineering the Luminescence and Generation of Individual Defect Emitters in Atomically Thin MoS₂. ACS Photonics **2021**, *8*, 669–677.
- (26) Stevens, C. E.; Chuang, H.-J.; Rosenberger, M. R.; McCreary, K. M.; Dass, C. K.; Jonker, B. T.; Hendrickson, J. R. Enhancing the Purity of Deterministically Placed Quantum Emitters in Monolayer WSe, ACS Nano 2022, 16, 20956–20963.
- (27) Wu, Z.; Luo, Z.; Shen, Y.; Zhao, W.; Wang, W.; Nan, H.; Guo, X.; Sun, L.; Wang, X.; You, Y.; Ni, Z. Defects as a Factor Limiting Carrier Mobility in WSe₂: A Spectroscopic Investigation. *Nano Res.* **2016**, *9*, 3622–3631.
- (28) Zhou, M.; Wang, W.; Lu, J.; Ni, Z. How Defects Influence the Photoluminescence of TMDCs. *Nano Res.* **2021**, *14*, 29–39.
- (29) Wu, Z.; Zhao, W.; Jiang, J.; Zheng, T.; You, Y.; Lu, J.; Ni, Z. Defect Activated Photoluminescence in WSe₂ Monolayer. *J. Phys. Chem. C* **2017**, *121*, 12294–12299.
- (30) Chow, P. K.; Jacobs-Gedrim, R. B.; Gao, J.; Lu, T.-M.; Yu, B.; Terrones, H.; Koratkar, N. Defect-Induced Photoluminescence in Monolayer Semiconducting Transition Metal Dichalcogenides. *ACS Nano* **2015**, *9*, 1520–1527.

- (31) Man, M. K. L.; Deckoff-Jones, S.; Winchester, A.; Shi, G.; Gupta, G.; Mohite, A. D.; Kar, S.; Kioupakis, E.; Talapatra, S.; Dani, K. M. Protecting the Properties of Monolayer MoS₂ on Silicon Based Substrates with an Atomically Thin Buffer. *Sci. Rep.* **2016**, *6*, 20890.
- (32) Watson, A. J.; Lu, W.; Guimarães, M. H. D.; Stöhr, M. Transfer of Large-Scale Two-Dimensional Semiconductors: Challenges and Developments. 2D Mater. 2021, 8, No. 032001.
- (33) Sharma, M.; Singh, A.; Aggarwal, P.; Singh, R. Large-Area Transfer of 2D TMDCs Assisted by a Water-Soluble Layer for Potential Device Applications. ACS Omega 2022, 7, 11731–11741.
- (34) Chae, W. H.; Cain, J. D.; Hanson, E. D.; Murthy, A. A.; Dravid, V. P. Substrate-Induced Strain and Charge Doping in Cvd-Grown Monolayer MoS₂. *Appl. Phys. Lett.* **2017**, *111*, No. 143106.
- (35) Zheng, C.; Xu, Z.-Q.; Zhang, Q.; Edmonds, M. T.; Watanabe, K.; Taniguchi, T.; Bao, Q.; Fuhrer, M. S. Profound Effect of Substrate Hydroxylation and Hydration on Electronic and Optical Properties of Monolayer MoS₂. *Nano Lett.* **2015**, *15*, 3096–3102.
- (36) Yu, Y.; Yu, Y.; Xu, C.; Cai, Y. Q.; Su, L.; Zhang, Y.; Zhang, Y.-W.; Gundogdu, K.; Cao, L. Engineering Substrate Interactions for High Luminescence Efficiency of Transition-Metal Dichalcogenide Monolayers. *Adv. Funct. Mater.* **2016**, *26*, 4733–4739.
- (37) Zhao, Y.; Xu, K.; Pan, F.; Zhou, C.; Zhou, F.; Chai, Y. Doping, Contact and Interface Engineering of Two-Dimensional Layered Transition Metal Dichalcogenides Transistors. *Adv. Funct. Mater.* **2017**, 27, No. 1603484.
- (38) Lien, D.-H.; Uddin, S. Z.; Yeh, M.; Amani, M.; Kim, H.; Ager, J. W.; Yablonovitch, E.; Javey, A. Electrical Suppression of All Nonradiative Recombination Pathways in Monolayer Semiconductors. *Science* **2019**, *364*, 468–471.
- (39) Qiu, Z.; Trushin, M.; Fang, H.; Verzhbitskiy, I.; Gao, S.; Laksono, E.; Yang, M.; Lyu, P.; Li, J.; Su, J.; Telychko, M.; Watanabe, K.; Taniguchi, T.; Wu, J.; Neto, A. H. C.; Yang, L.; Eda, G.; Adam, S.; Lu, J. Giant Gate-Tunable Bandgap Renormalization and Excitonic Effects in a 2D Semiconductor. *Sci. Adv.* **2019**, *5*, No. eaaw2347.
- (40) Baik, S.; Koo, Y.; Choi, W. Decreased N-Type Behavior of Monolayer MoS₂ Crystals Annealed in Sulfur Atmosphere. *Curr. Appl. Phys.* **2022**, *42*, 38–42.
- (41) Goodman, A. J.; Lien, D. H.; Ahn, G. H.; Spiegel, L. L.; Amani, M.; Willard, A. P.; Javey, A.; Tisdale, W. A. Substrate-Dependent Exciton Diffusion and Annihilation in Chemically Treated MoS₂ and WS₂. J. Phys. Chem. C **2020**, 124, 12175–12184.
- (42) Lin, Y.; Ling, X.; Yu, L.; Huang, S.; Hsu, A. L.; Lee, Y.-H.; Kong, J.; Dresselhaus, M. S.; Palacios, T. Dielectric Screening of Excitons and Trions in Single-Layer MoS₂. *Nano Lett.* **2014**, *14*, 5569–5576.
- (43) Harman, A. K.; Ninomiya, S.; Adachi, S. Optical Constants of Sapphire (α -Al₂O₃) Single Crystals. *J. Appl. Phys.* **1994**, *76*, 8032–8036.
- (44) Laturia, A.; Van de Put, M. L.; Vandenberghe, W. G. Dielectric Properties of Hexagonal Boron Nitride and Transition Metal Dichalcogenides: From Monolayer to Bulk. *npj 2D Mater. Appl.* **2018**, 2, 6.
- (45) Xiang, Y.; Sun, X.; Valdman, L.; Zhang, F.; Choudhury, T. H.; Chubarov, M.; Robinson, J. A.; Redwing, J. M.; Terrones, M.; Ma, Y.; Gao, L.; Washington, M. A.; Lu, T.-M.; Wang, G.-C. Monolayer MoS₂ on Sapphire: An Azimuthal Reflection High-Energy Electron Diffraction Perspective. 2D Mater. 2021, 8, No. 025003.
- (46) Eng, P. J.; Trainor, T. P.; Brown, G. E., Jr.; Waychunas, G. A.; Newville, M.; Sutton, S. R.; Rivers, M. L. Structure of the Hydrated Al₂O₃ (0001) Surface. *Science* **2000**, 288, 1029–1033.
- (47) Cochrane, K A; Zhang, T; Kozhakhmetov, A; Lee, J-H; Zhang, F; Dong, C; Neaton, J B; Robinson, J A; Terrones, M; Bargioni, A W.; Schuler, B Intentional Carbon Doping Reveals CH as an Abundant Charged Impurity in Nominally Undoped Synthetic WS₂ and WSe₂. 2D Mater. **2020**, 7, No. 031003.
- (48) Schuler, B.; Lee, J.-H.; Kastl, C.; Cochrane, K. A.; Chen, C. T.; Refaely-Abramson, S.; Yuan, S.; van Veen, E.; Roldán, R.; Borys, N. J.; Koch, R. J.; Aloni, S.; Schwartzberg, A. W.; Ogletree, D. F.; Neaton, J. B.; Weber-Bargioni, A. How Substitutional Point Defects in Two-

- Dimensional WS₂ Induce Charge Localization, Spin-Orbit Splitting, and Strain. ACS Nano 2019, 13, 10520-10534.
- (49) Azizi, A.; Wang, Y.; Stone, G.; Elias, A. L.; Lin, Z.; Terrones, M.; Crespi, V. H.; Alem, N. Defect Coupling and Sub-Angstrom Structural Distortions in $W_{1-x}Mo_xS_2$ Monolayers. *Nano Lett.* **2017**, 17, 2802–2808.
- (50) Huang, Y. L.; Chen, Y.; Zhang, W.; Quek, S. Y.; Chen, C.-H.; Li, L.-J.; Hsu, W.-T.; Chang, W.-H.; Zheng, Y. J.; Chen, W.; Wee, A. T. S. Bandgap Tunability at Single-Layer Molybdenum Disulphide Grain Boundaries. *Nat. Commun.* **2015**, *6*, 6298.
- (51) Zhou, W.; Zou, X.; Najmaei, S.; Liu, Z.; Shi, Y.; Kong, J.; Lou, J.; Ajayan, P. M.; Yakobson, B. I.; Idrobo, J.-C. Intrinsic Structural Defects in Monolayer Molybdenum Disulfide. *Nano Lett.* **2013**, *13*, 2615–2622.
- (52) Barja, S.; Refaely-Abramson, S.; Schuler, B.; Qiu, D. Y.; Pulkin, A.; Wickenburg, S.; Ryu, H.; Ugeda, M. M.; Kastl, C.; Chen, C.; Hwang, C.; Schwartzberg, A.; Aloni, S.; Mo, S.-K.; Ogletree, D. F.; Crommie, M. F.; Yazyev, O. V.; Louie, S. G.; Neaton, J. B.; Weber-Bargioni, A. Identifying Substitutional Oxygen as a Prolific Point Defect in Monolayer Transition Metal Dichalcogenides. *Nat. Commun.* **2019**, *10*, 3382.
- (53) Zhang, F.; Lu, Y.; Schulman, D. S.; Zhang, T.; Fujisawa, K.; Lin, Z.; Lei, Y.; Elias, A. L.; Das, S.; Sinnott, S. B.; Terrones, M. Carbon Doping of WS₂ Monolayers: Bandgap Reduction and P-Type Doping Transport. *Sci. Adv.* **2019**, *5*, No. eaav5003.
- (54) Greben, K.; Arora, S.; Harats, M. G.; Bolotin, K. I. Intrinsic and Extrinsic Defect-Related Excitons in TMDCs. *Nano Lett.* **2020**, 20, 2544–2550.
- (55) Mitterreiter, E.; Schuler, B.; Micevic, A.; Hernangómez-Pérez, D.; Barthelmi, K.; Cochrane, K. A.; Kiemle, J.; Sigger, F.; Klein, J.; Wong, E.; Barnard, E. S.; Watanabe, K.; Taniguchi, T.; Lorke, M.; Jahnke, F.; Finley, J. J.; Schwartzberg, A. M.; Qiu, D. Y.; Refaely-Abramson, S.; Holleitner, A. W.; Weber-Bargioni, A.; Kastl, C. The Role of Chalcogen Vacancies for Atomic Defect Emission in MoS₂. *Nat. Commun.* **2021**, *12*, 3822.
- (56) Wang, H.; Zhang, C.; Rana, F. Ultrafast Dynamics of Defect-Assisted Electron—Hole Recombination in Monolayer MoS₂. *Nano Lett.* **2015**, *15*, 339–345.
- (57) Sharma, M.; Singh, A.; Singh, R. Monolayer MoS₂ Transferred on Arbitrary Substrates for Potential Use in Flexible Electronics. *ACS Appl. Nano Mater.* **2020**, *3*, 4445–4453.
- (\$8) Mair, R. A.; Lin, J. Y.; Jiang, H. X.; Jones, E. D.; Allerman, A. A.; Kurtz, S. R. Time-Resolved Photoluminescence Studies of In_xGa_{1x}As_{1x}N_y. Appl. Phys. Lett. **2000**, 76, 188–190.
- (59) Baranowski, M.; Urban, J. M.; Zhang, N.; Surrente, A.; Maude, D. K.; Andaji-Garmaroudi, Z.; Stranks, S. D.; Plochocka, P. Static and Dynamic Disorder in Triple-Cation Hybrid Perovskites. *J. Phys. Chem.* C **2018**, *122*, 17473–17480.
- (60) Rogers, C.; Gray, D.; Bogdanowicz, N.; Mabuchi, H. Laser Annealing for Radiatively Broadened MoSe₂ Grown by Chemical Vapor Deposition. *Phys. Rev. Mater.* **2018**, *2*, No. 094003.
- (61) Cadiz, F.; Robert, C.; Wang, G.; Kong, W.; Fan, X.; Blei, M.; Lagarde, D.; Gay, M.; Manca, M.; Taniguchi, T.; Watanabe, K.; Amand, T.; Marie, X.; Renucci, P.; Tongay, S.; Urbaszek, B. Ultra-Low Power Threshold for Laser Induced Changes in Optical Properties of 2D Molybdenum Dichalcogenides. 2D Mater. 2016, 3, 045008.
- (62) Azzam, S. I.; Parto, K.; Moody, G. Prospects and Challenges of Quantum Emitters in 2D Materials. *Appl. Phys. Lett.* **2021**, *118*, 240502.